Summer Institute in Earth Sciences 2009

Algorithms for Spaceborne Weather Radar

The University of Maryland, Baltimore County
Department of Physics

Mentor: Robert Meneghini
NASA Goddard Space Flight Center

Abstract

The GPM satellite will include a dual-frequency radar to make more accurate precipitation measurements. By transmitting at two frequencies, the satellite will measure the dual frequency ratio in addition to the return power of both frequencies. The dual frequency ratio and the return power will allow a backwards recursion algorithm to calculate certain parameters of the drop size distribution. The problem with using two high frequencies is that the signals become attenuated. Although the nonlinear equations create sources of unknown error in the algorithm's output, they do account for the attenuation while calculating drop size distribution parameters. There are two main focuses of this study. One focus is to determine the reason for the errors we observe in the output and to create solutions to eliminate those errors. The second focus of this study is to expand the algorithm to include the other precipitation phases such as snow and melting layer.

1. Introduction

The Global Precipitation Measurement (GPM) mission is aimed towards obtaining more accurate data from spaceborne weather radar and increasing the types of information that can be retrieved. The GPM satellite, which is to be launched in 2013, will accomplish these goals by means of dual frequency radar. Currently, single frequency radar is able to observe the intensity and evolution of storms by measuring the reflectivity factor, Z, and calculating the precipitation rate, R, but the method is not perfect. The theory used to determine R from Z requires more information than what single frequency radar can provide, and has resulted in a number of Z-R relationships, each describing a different precipitation profile. The general form of the Z-R relationships is

$$Z = \alpha R^{\beta}$$

In order to decrease the variability that different meteorological conditions create, dual frequency radar transmits on bands that allow for Mie scattering, instead of Rayleigh scattering. Mie scattering occurs when the wavelength of the band is comparable in size to the particle, and Rayleigh scattering occurs when the wavelength is much larger than the particle. Single frequency ground-based radars usually transmit on the S (2 to 4 GHz) or C (4 to 8 GHz) band. The radar on the Tropical Rainfall Measurement Mission (TRMM) operates at Ku (13.8 GHz) band. For the most part, the Rayleigh approximation is valid for all three bands. If Mie scattering occurs at Ka band or both the Ku (13.6 GHz) and Ka (35.5 GHz) band, then certain drop size distribution (DSD) parameters can be derived from the reflectivity factors in a way that can not be determined by single frequency radar. However, a problem with using higher frequencies is that the attenuation of the signal increases.

A backward recursion algorithm is used to account for the attenuation at the Ka and Ku band, while it calculates the DSD parameters from the measured reflectivity factors. This algorithm is prone to error because it uses nonlinear equations to account for the different variables and to correct for attenuation. The main goal of this study is to discover the sources of error in the algorithm and to expand the algorithm to account for different meteorological conditions.

2. Background

a. *Gamma distribution of particle size*

Raindrops, snowflakes, and other meteorological particles have drop size distributions that are characterized very well by the Gamma distribution. The Gamma distribution is

$$N(D) = N_0 D^{\mu} e^{-\Lambda D}$$

where D (mm) is the drop diameter, N (m^{-3} mm^{-1}) is the number of drops with a certain diameter per unit volume; this quantity is often referred to the drop size distribution (DSD). The N_0 (m^{-3} $mm^{-\mu-1}$) is the coefficient of the DSD, and μ is the shape factor of the distribution. In order to compute N(D), it is convenient to define the quantity N_T (m^{-3}), which is the number concentration per unit volume. The N_T can be obtained by integrating the DSD from zero to infinity:

$$N_T = \int_0^\infty N(D)dD = \frac{N(D)}{n(D)}$$

where

$$n(D) = \frac{\Lambda^{\mu+1} D^\mu e^{-\Lambda D}}{\Gamma(\mu+1)}$$

The n (mm^{-1}) is known as the normalized size distribution. The Γ or Gamma function in the n is defined by

$$\Gamma(x) = \int_0^\infty t^{x-1} e^{-t} dt$$

For integer values of μ, the Γ function can be written as a factorial:

$$\Gamma(\mu+1) = \int_0^\infty t^\mu e^{-t} dt = \mu!$$

If we rearrange the solution of the integral, N becomes

$$N(D) = N_T n(D)$$

or

$$N(D) = \frac{N_T \Lambda^{\mu+1} D^\mu e^{-\Lambda D}}{\Gamma(\mu+1)}$$

The quantity Λ can be described in two ways. One way is to describe Λ in terms of D_0 (mm), which is the median mass diameter. More specifically, the median mass diameter is the diameter that divides the drop size distribution into two equal parts, each containing half of the total water content. The expression for Λ in terms of D_0 is

$$\Lambda = \frac{3.67 + \mu}{D_0}$$

The second way to describe Λ is in terms of D_m (mm) or the mean diameter. The mean diameter is actually the ratio between the fourth and third moment of the DSD.

$$D_m = \frac{\int_0^\infty D^4 N(D) dD}{\int_0^\infty D^3 N(D) dD}$$

The expression for Λ in terms of D_m is

$$\Lambda = \frac{4.00 + \mu}{D_m}$$

b. *Relation between radar and precipitation measurements*

The radar equation relates the return power, which is the physical quantity measured by the radar, to the measured reflectivity factor, which is associated with the DSD parameters described above. The radar equation is

$$P_r = \frac{C|K|^2 Z_m}{r^2}$$

where P_r is the return power, C is the radar constant, which depends on the specifications of the radar, K is the dielectric factor of water, Z_m ($mm^6\ m^{-3}$) is the measured reflectivity factor, and r (km) or range is the distance from the radar. The radar equation helps to determine N_T in the algorithm, however D_0 must be found before N_T can be calculated.

The method to solve for D_0 and N_T will be described in more detail in the algorithm section, but there are several relevant equations to the algorithm that will be described here. One of these equations describes the Z_m in terms of the true reflectivity factor Z ($mm^6\ m^{-3}$) and the attenuation A:

$$Z_m(r,\lambda) = Z(r,\lambda)A(r,\lambda)$$

Another relevant equation that describes the true reflectivity factor is

$$Z(r,\lambda) = \frac{\lambda^4}{\pi^5 |K|^2} \int_0^\infty \sigma_b(\lambda,D) N(D) dD$$

where λ (mm) is the radar wavelength and σ_b (mm^2) is the backscattering cross section. If the number concentration and the normalized size distribution are substituted in for the DSD, then

$$Z(r,\lambda) = \frac{\lambda^4}{\pi^5 |K|^2} N_T \int_0^\infty \sigma_b(\lambda,D) n(D) dD$$

$$Z(r,\lambda) = \frac{\lambda^4}{\pi^5 |K|^2} N_T I_b(\lambda,\Lambda)$$

The I_b ($mm^{7+\mu}$) is the backscattering integral equation and can be explicitly described as

$$I_b(\lambda,\Lambda) = \int_0^\infty \sigma_b(\lambda,D) n(D) dD$$

The I_b is important because it relates to a physical quantity measured by the radar, the dual frequency ratio (DFR). The definition of the DFR is

$$DFR = \frac{Z(r,\lambda_1)}{Z(r,\lambda_2)}$$

The DFR is related to the I_b by the equation

$$DFR = \frac{I_b(\lambda_1,\Lambda)}{I_b(\lambda_2,\Lambda)}$$

The DFR allows the algorithm another measured physical quantity other than the return power to calculate the DSD parameters.

c. *Attenuation*

The presence of attenuation complicates the radar retrieval because it accumulates and becomes larger as the signal propagates through the storm. Atmospheric gases, clouds, snow, rain, and other hydrometeors can cause attenuation. For signals transmitted at Ku and Ka-bands, the attenuation by gases, clouds, and snow is usually negligible, but

the attenuation from the melting layer and the rain needs to be taken into account. The attenuation that reduces Z to Z_m can be expressed as

$$A(r,\lambda) = e^{-0.2\ln 10\int_0^r k(\lambda,s)ds}$$

where k (dB km^{-1}) is attenuation coefficient, which describes the loss in the signal's intensity due to scattering and absorption by hydrometeors. To determine attenuation coefficient, the extinction cross section σ_e (mm^2) must be multiplied by the DSD and integrated over all sizes. The equation for k is

$$k(\lambda) = \int_0^\infty \sigma_e(\lambda,D)N(D)dD$$

If the number concentration and the normalized size distribution are substituted in for the DSD, then

$$k(\lambda) = N_T \int_0^\infty \sigma_e(\lambda,D)n(D)dD$$

$$k(\lambda) = N_T I_e(\lambda,\Lambda)$$

where I_e (dB $mm^{\mu+1}$ m^3 km^{-1}) is the extinction integral equation. The I_e will become critical in calculating the attenuation at each range gate.

$$I_e(\lambda,\Lambda) = \int_0^\infty \sigma_e(\lambda,D)n(D)dD$$

3. Data Retrieval Program

a. *Main program (Robert Meneghini and Liang Lao wrote the program.)*

The data retrieval program used to determine the DSD parameters employs a backwards recursion algorithm to account for the attenuation at a specific height, while calculating the parameters of the drop size distribution (D_0, N_T) at that height. Conventional radars operate by transmitting a short pulse of length τ and then receiving the power that is backscattered to the antenna. A particular range gate corresponds to the time delay between transmission and reception and where the gate length, h, is equal to $c\tau/2$ where c is the speed of light. If the full range within the atmosphere is divided into n such gates the program can calculate D_0, N_T, and specific attenuation for each of the

gates. At the last or nth gate, closest to the surface the attenuation will be at maximum. The first gate is the gate closest to the radar and is known as gate zero. At gate zero, there is no attenuation. The top of a storm is considered gate zero in practice because the attenuation accumulated by the atmospheric gases and other clouds are negligible. Either way, the first gate should have no attenuation.

The program proceeds through the steps describe below to find the DSD parameters and the specific attenuation at each gate.

1. Opens the file containing the experimental or simulated data at both frequencies. Experimental data was retrieved by dual frequency radar on an airplane. Also, a separate program can create simulated data by assuming a D_0 and a N_T and calculating the Z_m at each range gate.

2. Opens the look-up tables for both frequencies. A separate program creates the look-up tables at a specific frequency and precipitation with a constant μ, a constant temperature, and a constant elevation. The table consist of I_b and I_e values for 700 D_0 values from 0.2 mm to 4.0 mm.

3. Runs the backward recursion algorithm.

4. Outputs a data file containing the D_0, N_T, and rain rate R at every range gate.

b. *Backwards Recursion Algorithm*

The recursion subroutine makes some assumptions, while it calculates the DSD parameters. One assumption is that μ, the shape parameter of the distribution, is a constant through all the range gates along the radar beam. Another assumption involves the total path-integrated attenuation (PIA) or the attenuation out to the n*th* gate. There are two methods to approximate the PIA. One method is the surface reference technique, which estimates the total PIA by comparing the surface return of a precipitation-free area to the surface return within the storm. If the surface cross sections are the same, then the ratio of these two measurements is equal to the total PIA. The other method is the soft constraint method, which assumes a range of D_0 values at the last gate and uses those assumed values to calculate the PIA. The shortcoming of this method is that the data retrieval program will produce multiple solutions, one for each assumed D_0 value. A third assumption is that the DFR as a function of D_0 does not change with temperature or that the temperature change with the height is known.

The steps below describe the backwards recursion algorithm and the details at each step.

1. For gate n, calculate the Z_m from the P_r for both frequencies by rearranging the radar equation.

$$Z_m(r_n,\lambda) = \frac{r^2 P_r}{C|K|^2}$$

2. Determine the DFR with the Z_m and the PIA approximation for both frequencies.

$$DFR = \frac{Z(r_n,\lambda_1)}{Z(r_n,\lambda_2)}$$

$$DFR = \frac{Z_m(r_n,\lambda_1)/A(r_n,\lambda_1)}{Z_m(r_n,\lambda_2)/A(r_n,\lambda_2)}$$

3. Create a polynomial fit of the DFR as a function of D_0, and find the D_0 for gate n. The DFR as a function of D_0 is known, which is why it can be fit to a curve. The figure below shows the function with different μ values.

Figure 1

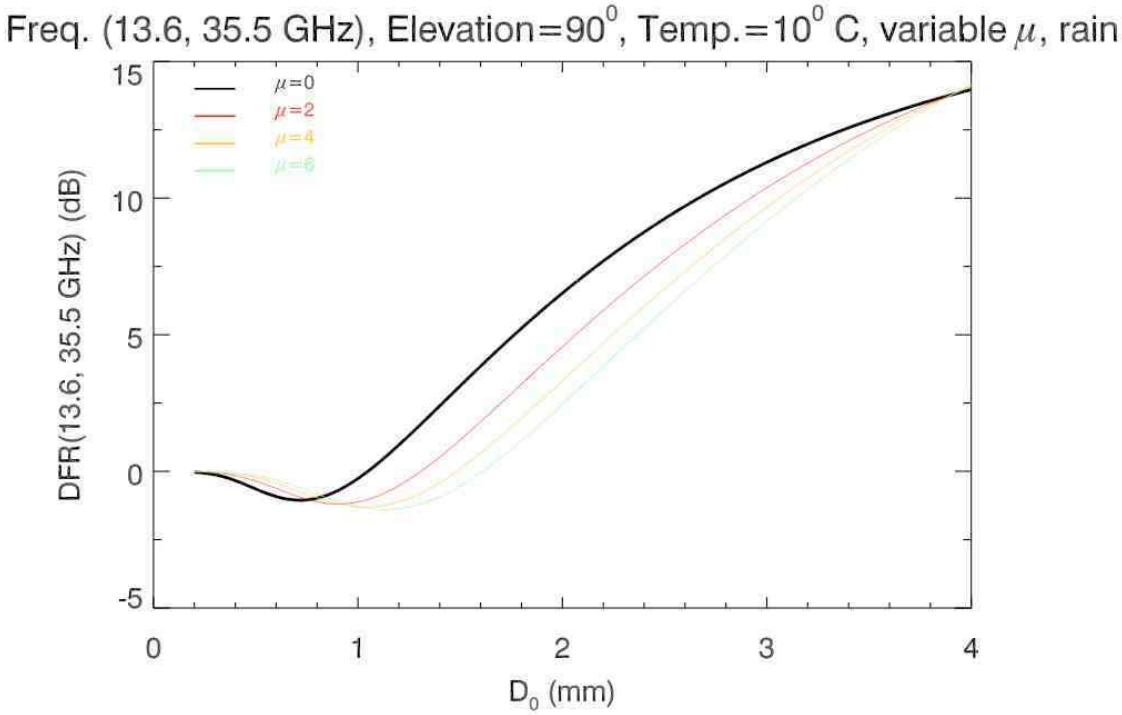

4. Search the look-up table for the D_0 that corresponds to the estimated DFR. If the D_0 found by the fit does not match exactly with any of the D_0 values found in the table, then use a linear interpolation to determine the D_0 value. The look-up table will also provide the I_b and the I_e for the last range gate.

5. Determine Λ from the calculated D_0 value and the set μ values.

$$\Lambda = \frac{3.67 + \mu}{D_0}$$

6. Calculate N_T by rearranging the equation for the true reflectivity factor. All of the values needed to calculate the N_T are either known or set constants.

$$Z(r_n, \lambda) = \frac{\lambda^4}{\pi^5 |K|^2} N_T I_b(\lambda, \Lambda)$$

$$N_T = \left[\frac{\pi^5 |K|^2}{\lambda^4}\right]\left[\frac{Z_m(r_n, \lambda)}{A(r_n, \lambda) I_b(\lambda, \Lambda)}\right]$$

7. Find the specific attenuation at gate n with the values for N_T and I_e.

$$k_n(\lambda) = N_T I_e(\lambda, \Lambda)$$

8. Determine the attenuation at gate n-1 with the specific attenuation at gate n.

$$A(r_{n-1}, \lambda) = e^{-0.2 \ln 10 h \int_0^{r_n} k(\lambda, s) ds}$$

$$A(r_{n-1}, \lambda) = e^{-0.2 \ln 10 h \int_0^{r_n} \left[k_{PIA}(\lambda, s) - k_n(\lambda, s)\right] ds}$$

9. Repeat steps 1 through 7 for gate n-1 and use the attenuation at gate n-1 instead of the PIA approximation.

10. Determine the attenuation at gate n-2 with the specific attenuation at gate n-1.

$$A(r_{n-2}, \lambda) = e^{-0.2 \ln 10 h \int_0^{r_n} \left[k_{PIA}(\lambda, s) - k_n(\lambda, s) - k_{n-1}(\lambda, s)\right] ds}$$

11. Repeat steps 9 and 10 until the D_0 and N_T at each range gate are found.

4. Discrepancies in the DFR

a. *The Shape Factor, μ*

The DFR as a function of D_0 is not the same for all values of μ. This can be seen in Figure 1. To check how μ changes the solutions produced by the data retrieval program, the simulated data set is created first with a specific μ value, usually μ equal to two. Then the program is executed with different assumed μ values. From Figure 1, we can determine how the difference between the actual μ of the simulated data and the assumed μ in the program will affect the solutions. The DFRs show us that if the actual μ is greater than the assumed μ, then the D_0 values are underestimated and the N_0 values are overestimated. This can be seen in Figure 2a, where the black line is the correct solution and the colored lines are the multiple solutions produced by the soft constraint method. The DFRs also show us that if the actual μ is less than the assumed μ, then the D_0 values are overestimated and the N_T values are underestimated. This is illustrated in Figures 2c and 2d. Figure 2b just shows us the solutions for the control case, where the assumed μ equal to the actual μ.

An interesting side note is that rain rate R is not over or underestimated. The reason behind this is that the D_0 values are changing inversely to the N_T values. Thus, the change in D_0 and the inverse change in N_T leaves R relatively unaffected.

Figure 2a

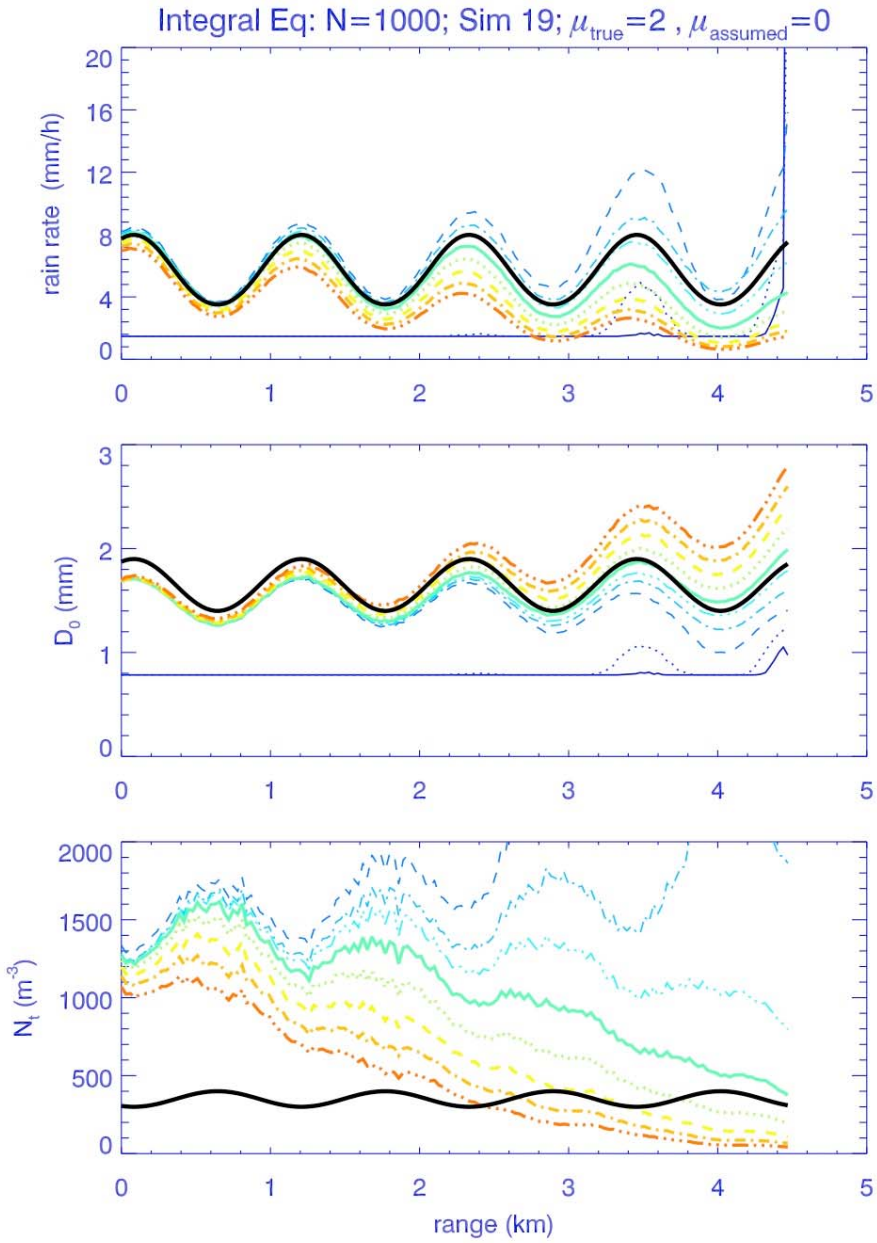
Integral Eq: N=1000; Sim 19; μ_{true}=2 , $\mu_{assumed}$=0
rain rate (mm/h)
D_0 (mm)
N_t (m^{-3})
range (km)

Figure 2b

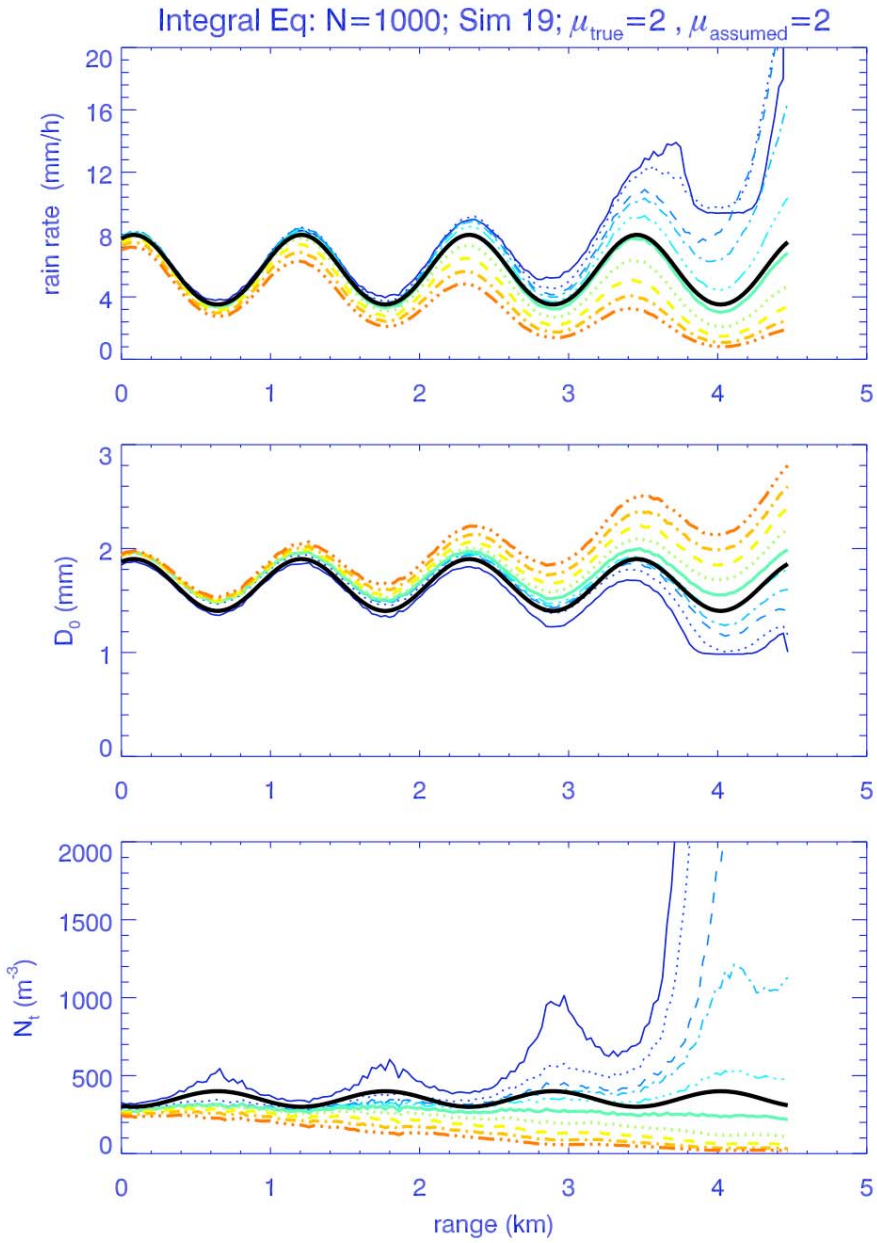
Integral Eq: N=1000; Sim 19; μ_{true}=2 , $\mu_{assumed}$=2
rain rate (mm/h)
D_0 (mm)
N_t (m^{-3})
range (km)

Figure 2c

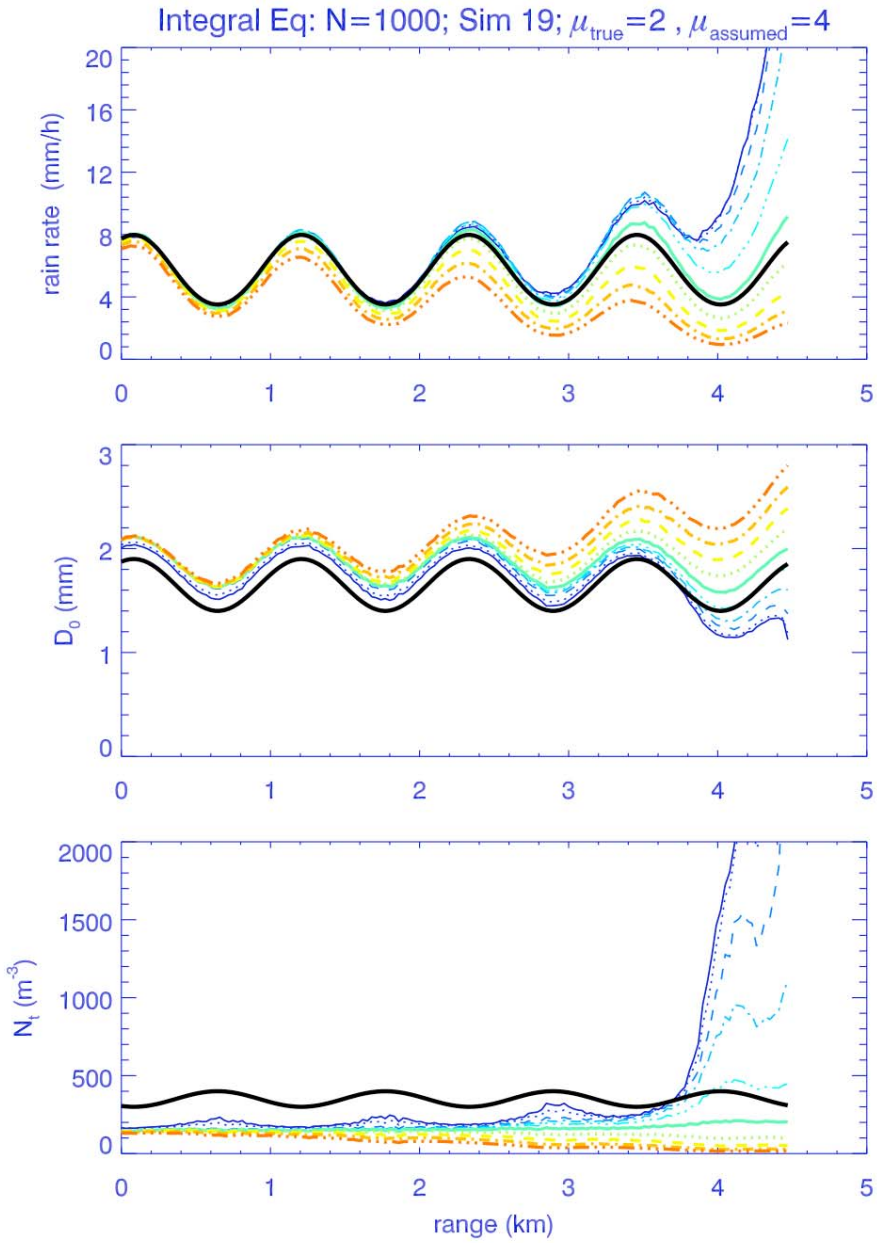
Integral Eq: N=1000; Sim 19; μ_{true}=2 , $\mu_{assumed}$=4
rain rate (mm/h)
D_0 (mm)
N_t (m^{-3})
range (km)

Figure 2d

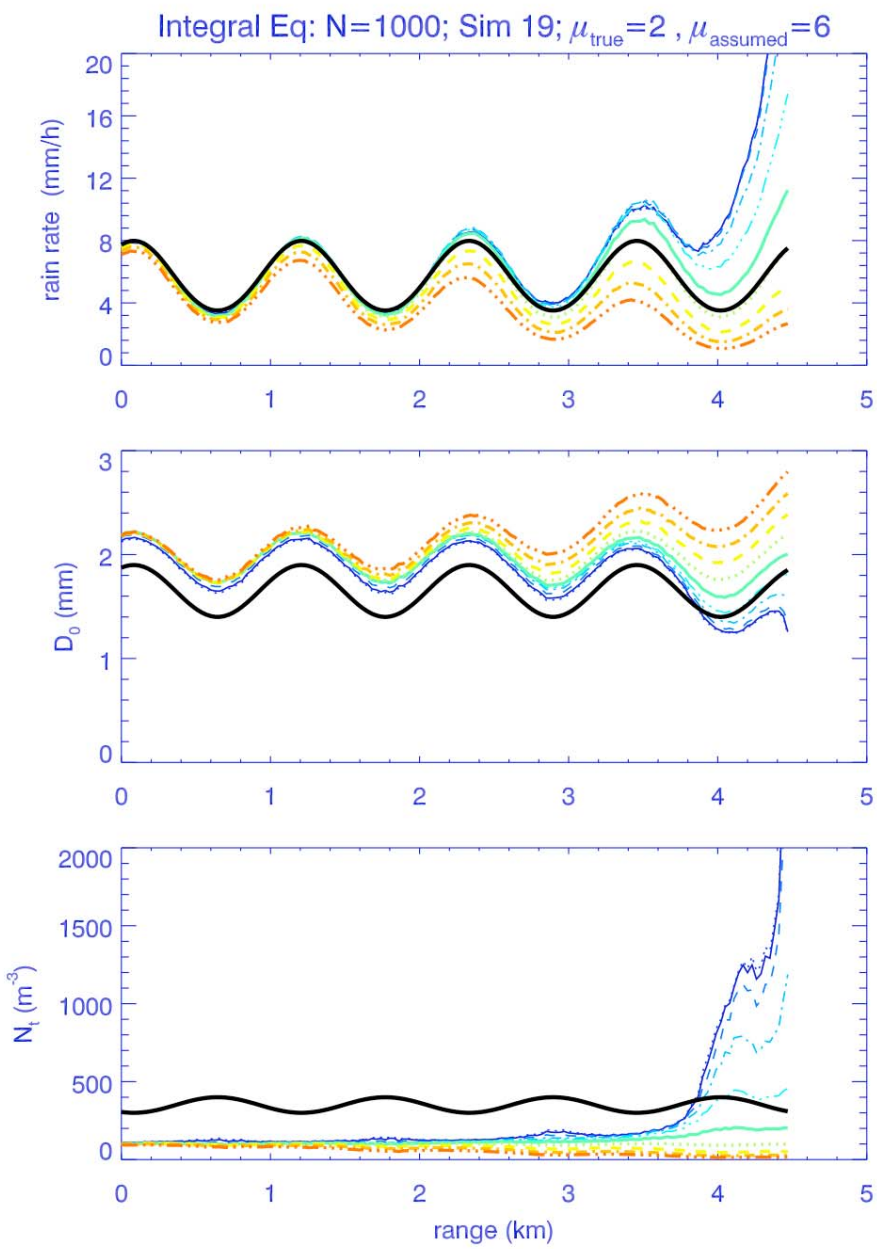

b. *The Dielectric Constant, K*

The dielectric constant can be calculated theoretically as function of frequency or can be approximated by the value 0.93. Either convention can be used in the calculation of the DFR, but there is an offset between the DFRs of the two conventions. The DFRs

are shown in Figure 3. While there is a difference in the DFRs of the two conventions, the data retrieval program could use either convention without significantly impacting the solutions.

Figure 3

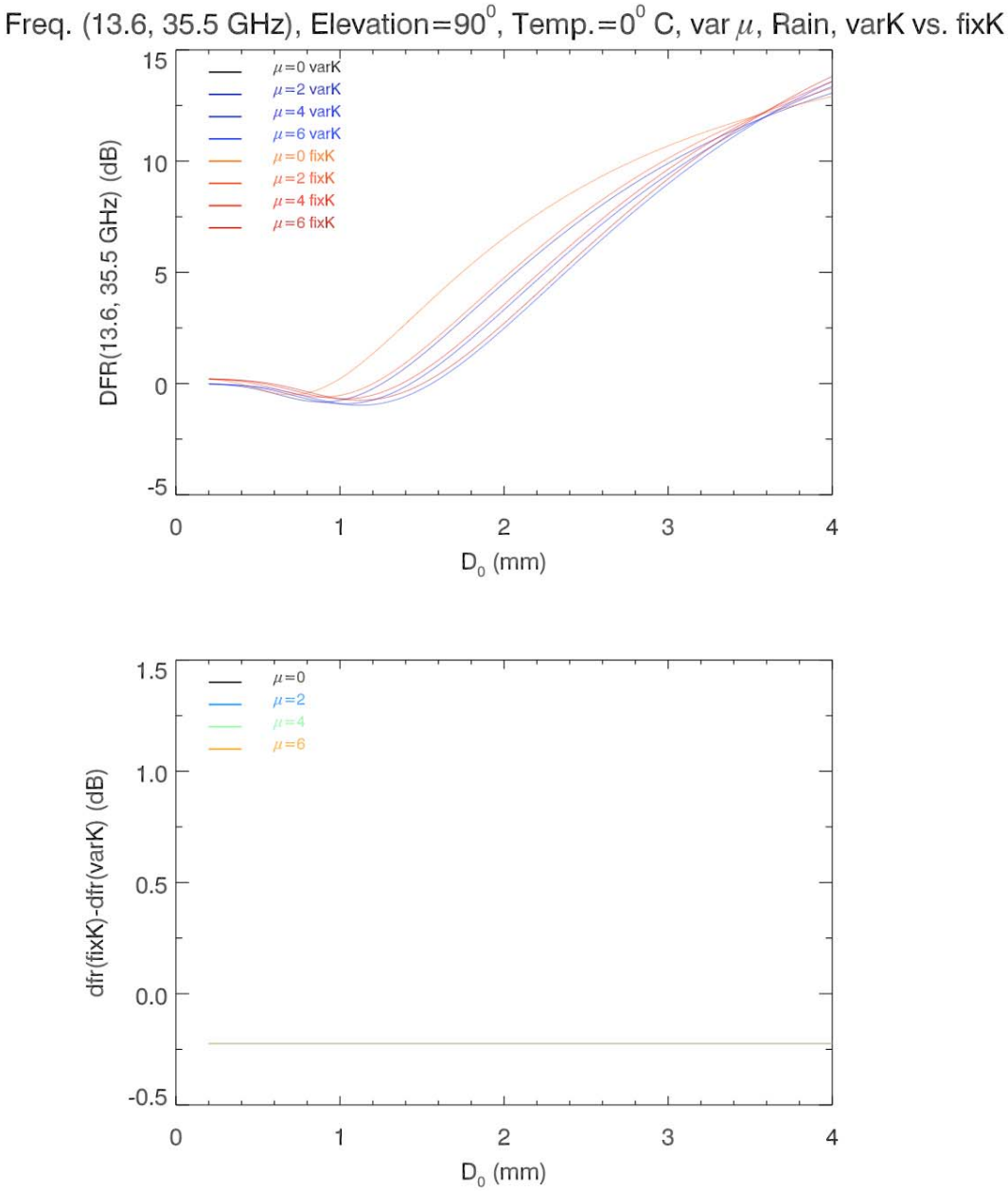

c. *The Air Temperature*

Previously, we thought that there would very little change in the DFRs at different air temperatures. That is largely true, but Figure 4 shows us that as the temperature decreases, the DFR minimum decreases. The solutions produced by the data retrieval program are not affected significantly because for most values of D_0 and DFR the relationship does not change with temperature.

Figure 4

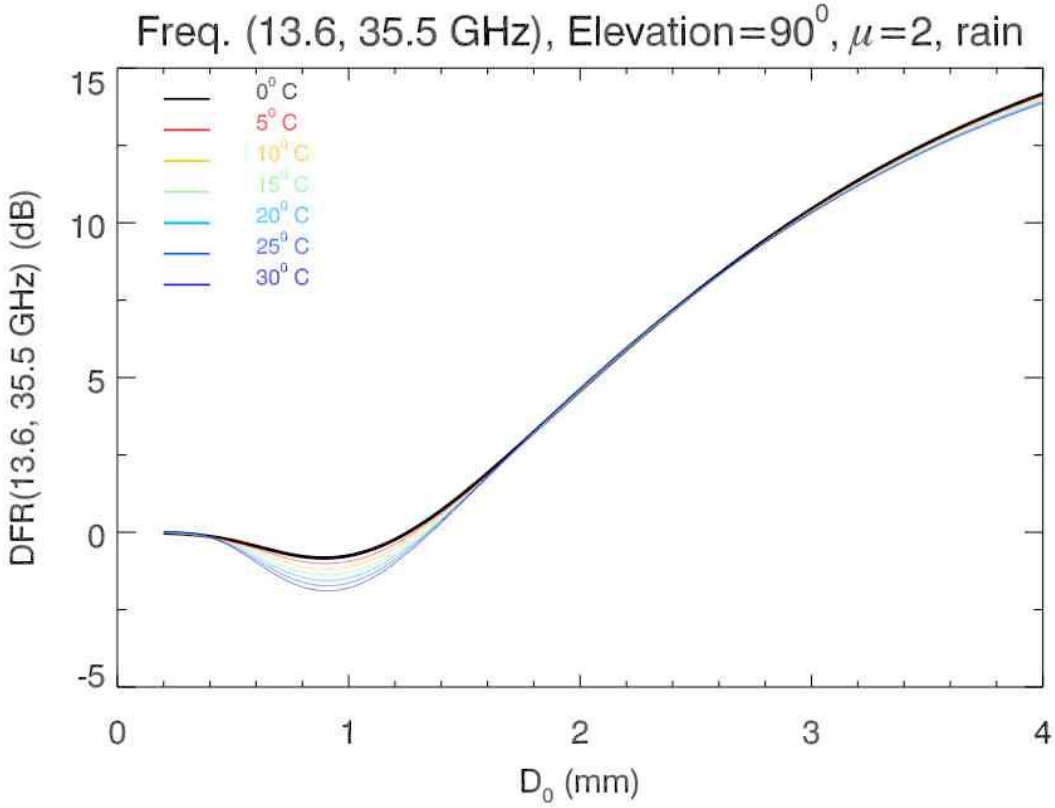

5. Errors in the Data Retrieval Program

The only serious error we encountered in the data retrieval program occurred when N_T was very large. Figure 5 shows us the results of such a situation. In the figure, the calculated D_0, N_T, and R values are not remotely similar to the true values. We believe that the error is a result of losing the Ka band in the simulated precipitation because a large N_T usually means there is a large water-content. A large water-content could attenuate the signal on the Ka band enough to diminish it completely. Figures 6a through 6d shows us how the model degenerates as N_T increases. Even though the errors associated with the data retrieval program are significant, the program can still be used to analyze real experimental data because the very large N_T values used in the simulation are unlikely in actual rain.

Figure 5

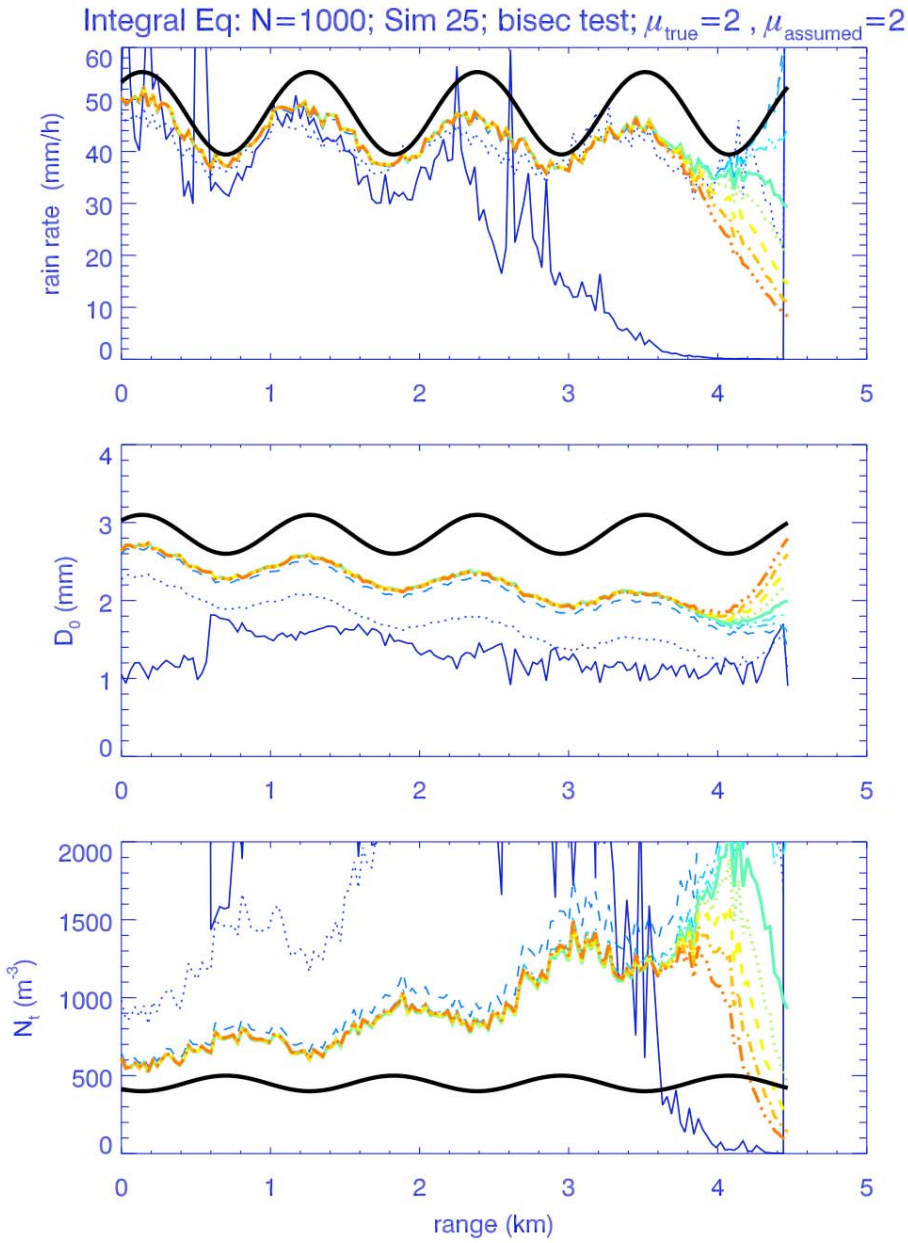
Integral Eq: N=1000; Sim 25; bisec test; μ_{true}=2 , $\mu_{assumed}$=2
rain rate (mm/h)
D_0 (mm)
N_t (m^{-3})
range (km)

Figure 6a

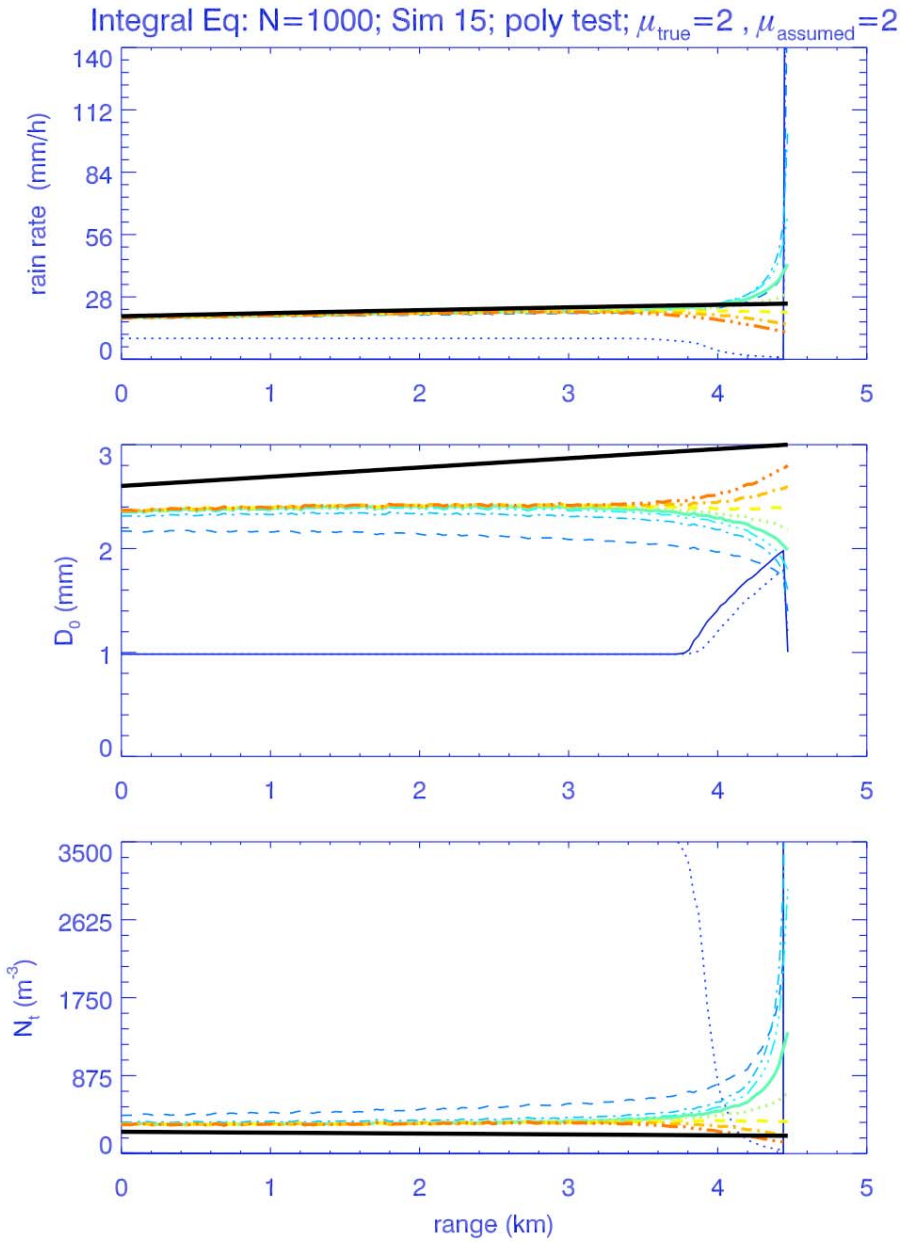
Integral Eq: N=1000; Sim 15; poly test; μ_{true}=2 , $\mu_{assumed}$=2
rain rate (mm/h)
140
112
84
56
28
0
0
1
2
3
4
5
D_0 (mm)
3
2
1
0
N_t (m^{-3})
3500
2625
1750
875
range (km)

Figure 6b

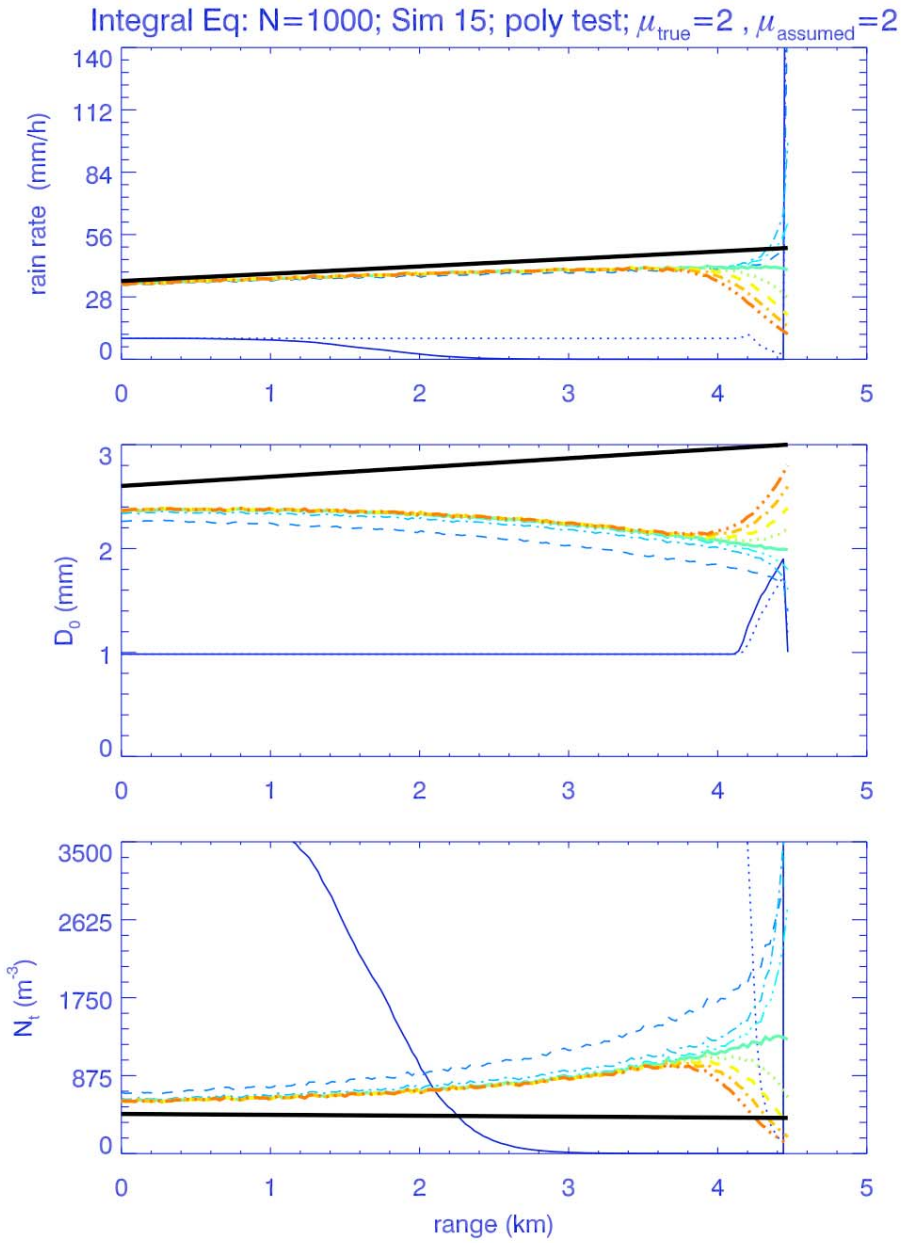
Integral Eq: N=1000; Sim 15; poly test; μ_{true}=2 , $\mu_{assumed}$=2
rain rate (mm/h)
140
112
84
56
28
0
0
1
2
3
4
5
D_0 (mm)
3
2
1
0
N_t (m^{-3})
3500
2625
1750
875
0
range (km)

Figure 6c

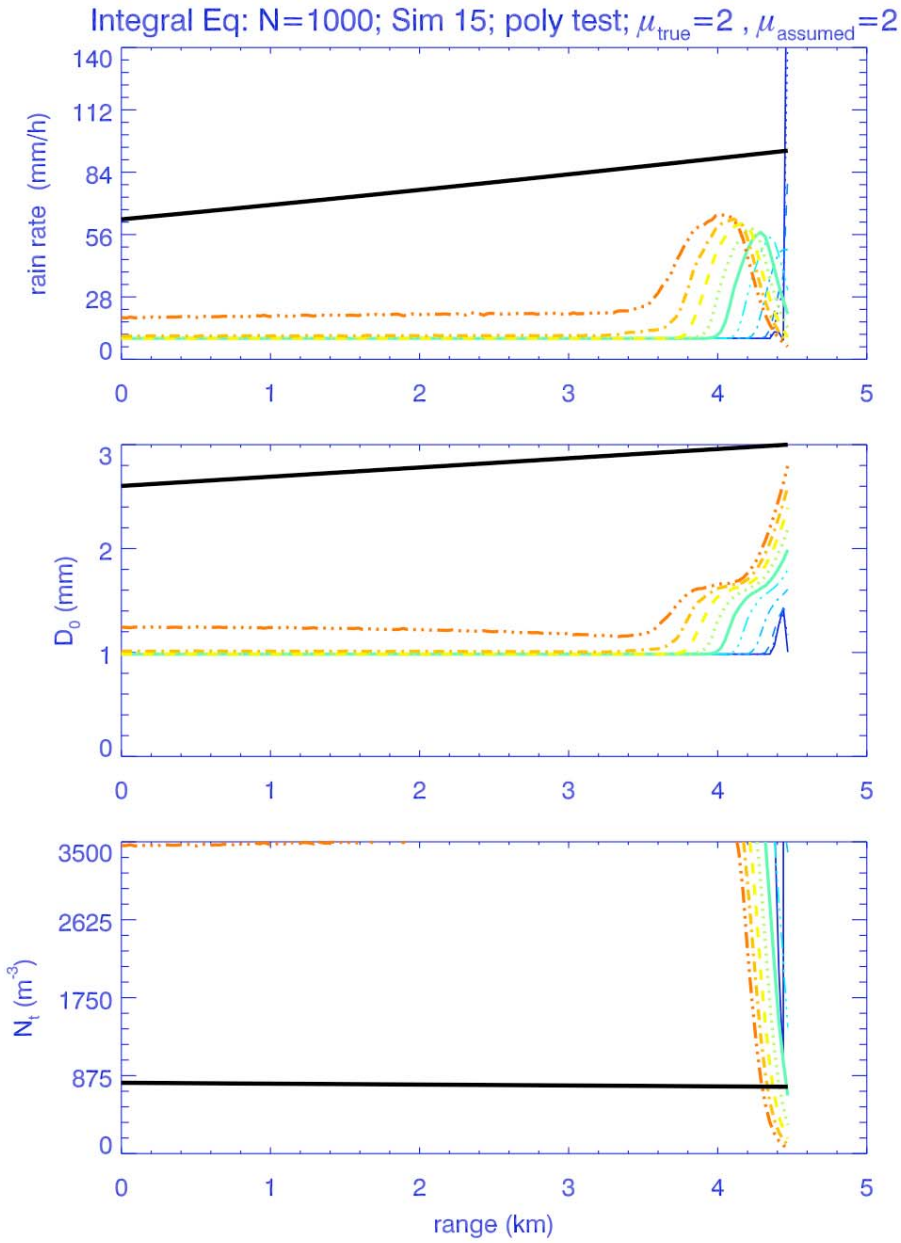
Integral Eq: N=1000; Sim 15; poly test; μ_{true}=2 , $\mu_{assumed}$=2
rain rate (mm/h)
140
112
84
56
28
0
0
1
2
3
4
5
D_0 (mm)
3
2
1
0
N_t (m^{-3})
3500
2625
1750
875
0
range (km)

Figure 6d

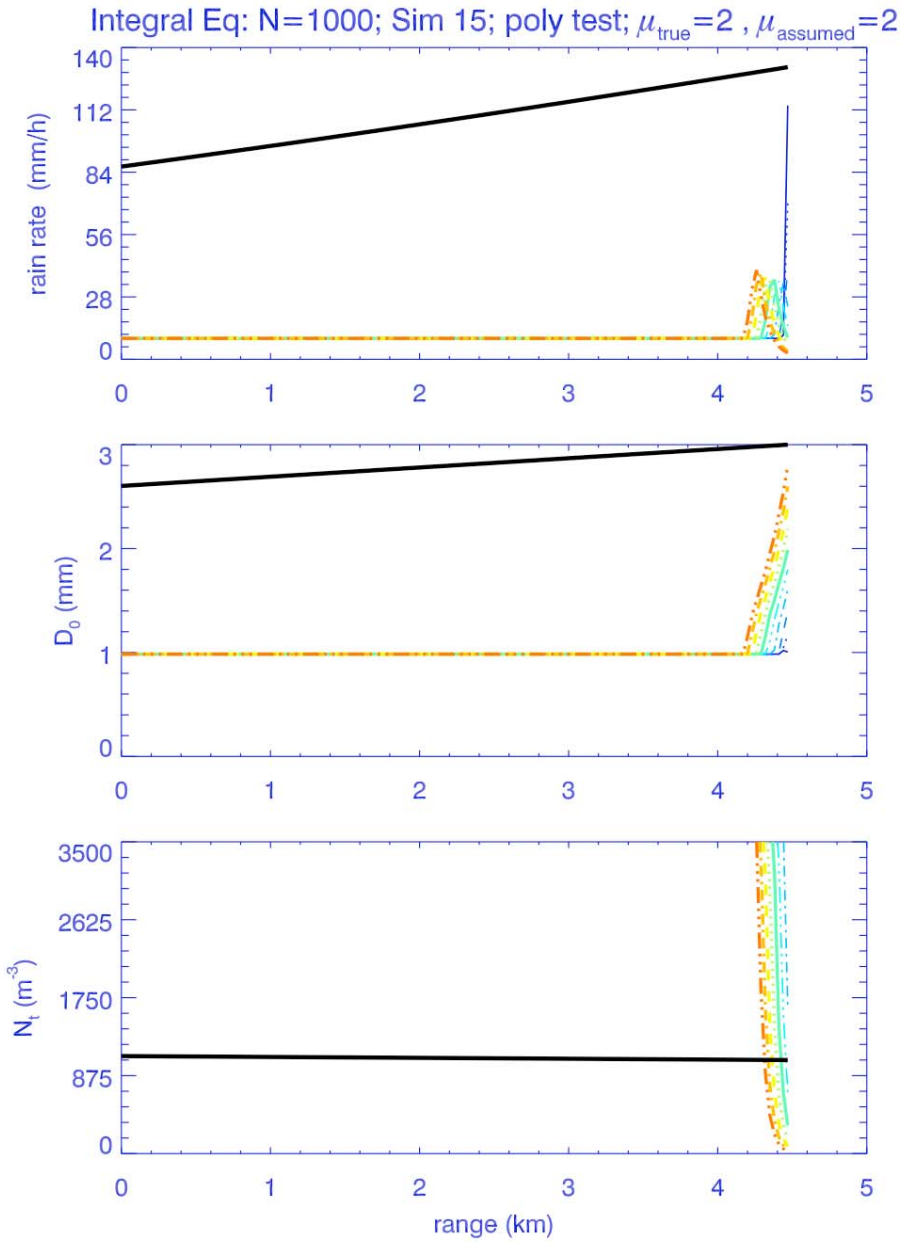
Integral Eq: N=1000; Sim 15; poly test; μ_{true}=2 , $\mu_{assumed}$=2
rain rate (mm/h)
140
112
84
56
28
0
0
1
2
3
4
5
D_0 (mm)
3
2
1
0
N_t (m^{-3})
3500
2625
1750
875
0
range (km)

6. Expanding the Data Retrieval Program

a. *The Snow DFRs*

The DFR-D0 relationship for snow is different than the DFR-D0 relationship for rain, which is why separate look-up tables are needed for snow. One difference is that all the DFRs of snow can be approximated well by assuming μ is equal to zero. However, the DFR of snow does depend on the snow density ρ (g cm^{-3}). Another difference is that when we calculate the DFR of snow, we determine the DFR as a function of D_0 snow, instead of D_0 liquid water. Figure 7 shows us the DFR of snow as a function of D_0 liquid water, which is a convention used by the rain and melting layer look-up tables.

Figure 7

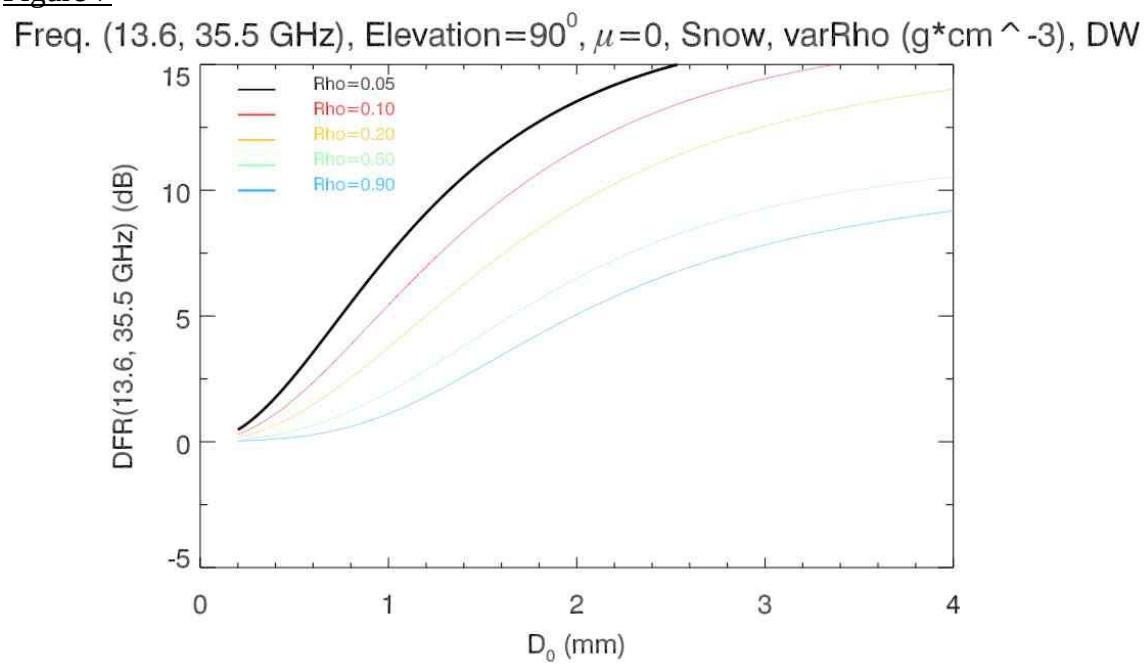

b. *The Melting Layer*

For the melting layer, which is also known as the bright band, the DFR changes from a snow DFR at the 0° C isotherm to a rain DFR at some lower height. We created the bright band look-up tables by integrating the DSD multiplied by the backscattering cross sections from the smallest to the largest particle diameter. The integration was done at 60 different heights. Figure 9 is a visualization of the calculations. The bright band look-up table contains 700 D_0 for each of the 60 range gates, which results in 42000 I_b and I_e values. Figure 8 shows us the DFRs at each range gate in the melting layer and illustrates how the DFRs transition from snow to rain.

Figure 8

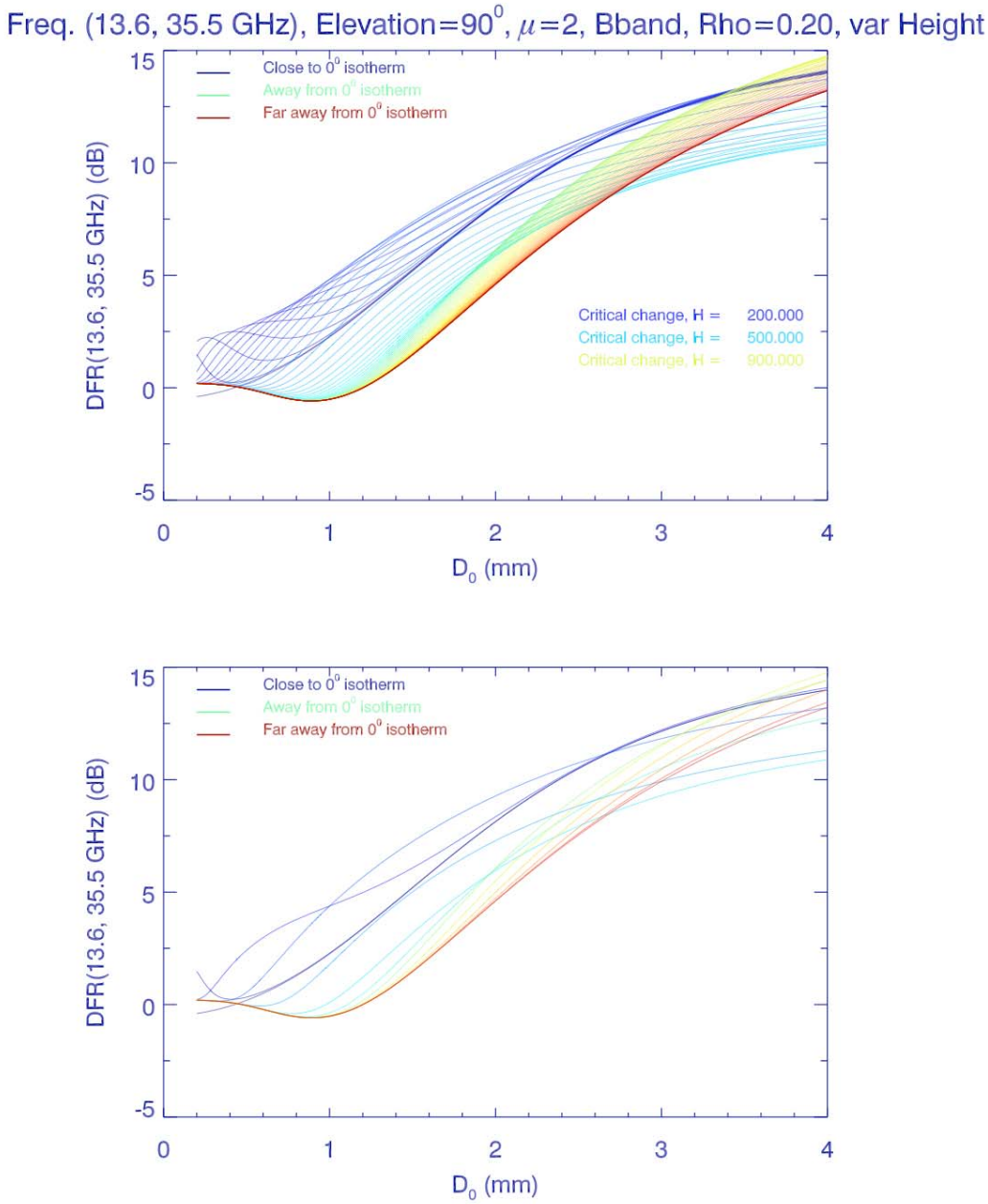
Freq. (13.6, 35.5 GHz), Elevation=90^0, μ=2, Bband, Rho=0.20, var Height
Close to 0^0 isotherm
Away from 0^0 isotherm
Far away from 0^0 isotherm
Critical change, H = 200.000
Critical change, H = 500.000
Critical change, H = 900.000
DFR(13.6, 35.5 GHz) (dB)
D$_0$ (mm)
Close to 0^0 isotherm
Away from 0^0 isotherm
Far away from 0^0 isotherm
DFR(13.6, 35.5 GHz) (dB)
D$_0$ (mm)

Figure 9

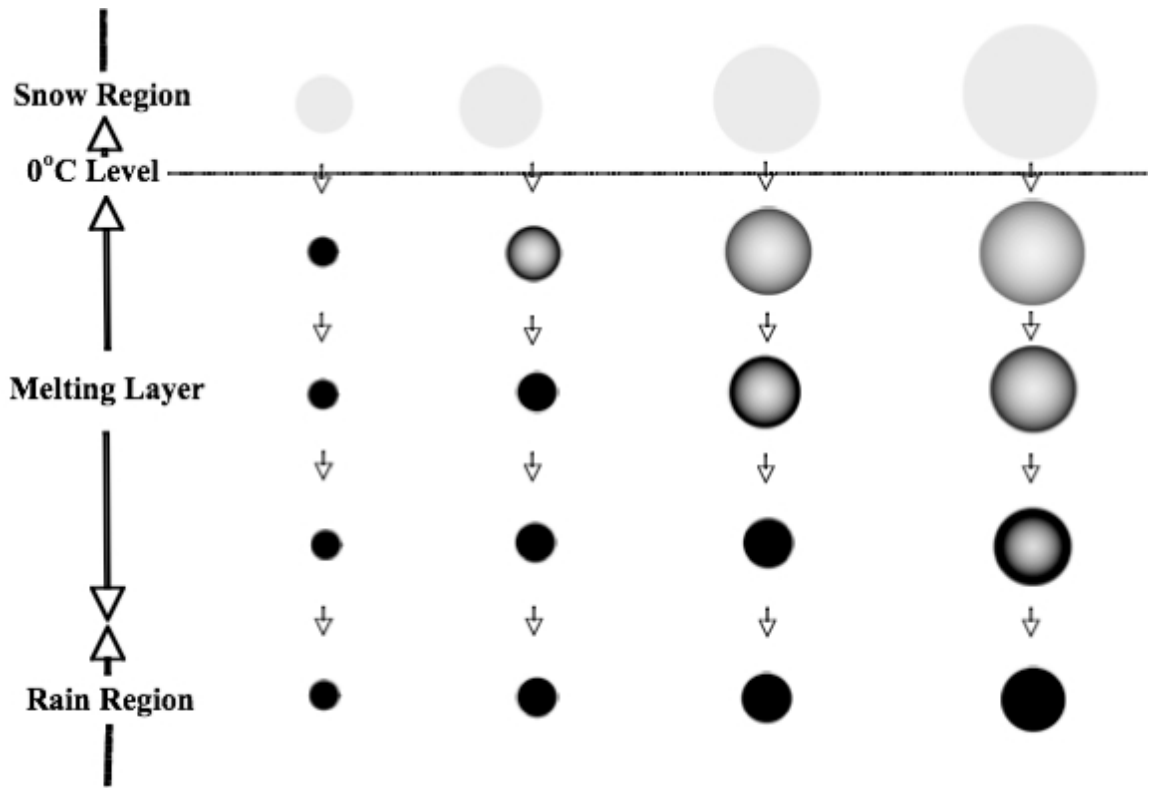

A comparison between the look-up tables we created revealed that there are some discrepancies between the tables. At the lowest range gate in the bright band table, the DFR is supposed to match the DFR of the rain table exactly because at the lowest range gate the drops have all melted into water. As can be seen in Figure 10, there are discrepancies between the two tables. At the highest range gate in the bright band table, the DFR is supposed to match the DFR of the snow tables. As can be seen in Figure 11, there are also discrepancies between the snow table and the bright band table. The discrepancies in the snow table are particularly disturbing because it seems that they depend on the snow density, but the discrepancies do not do increase or decrease as the density increases or decreases.

Figure 10

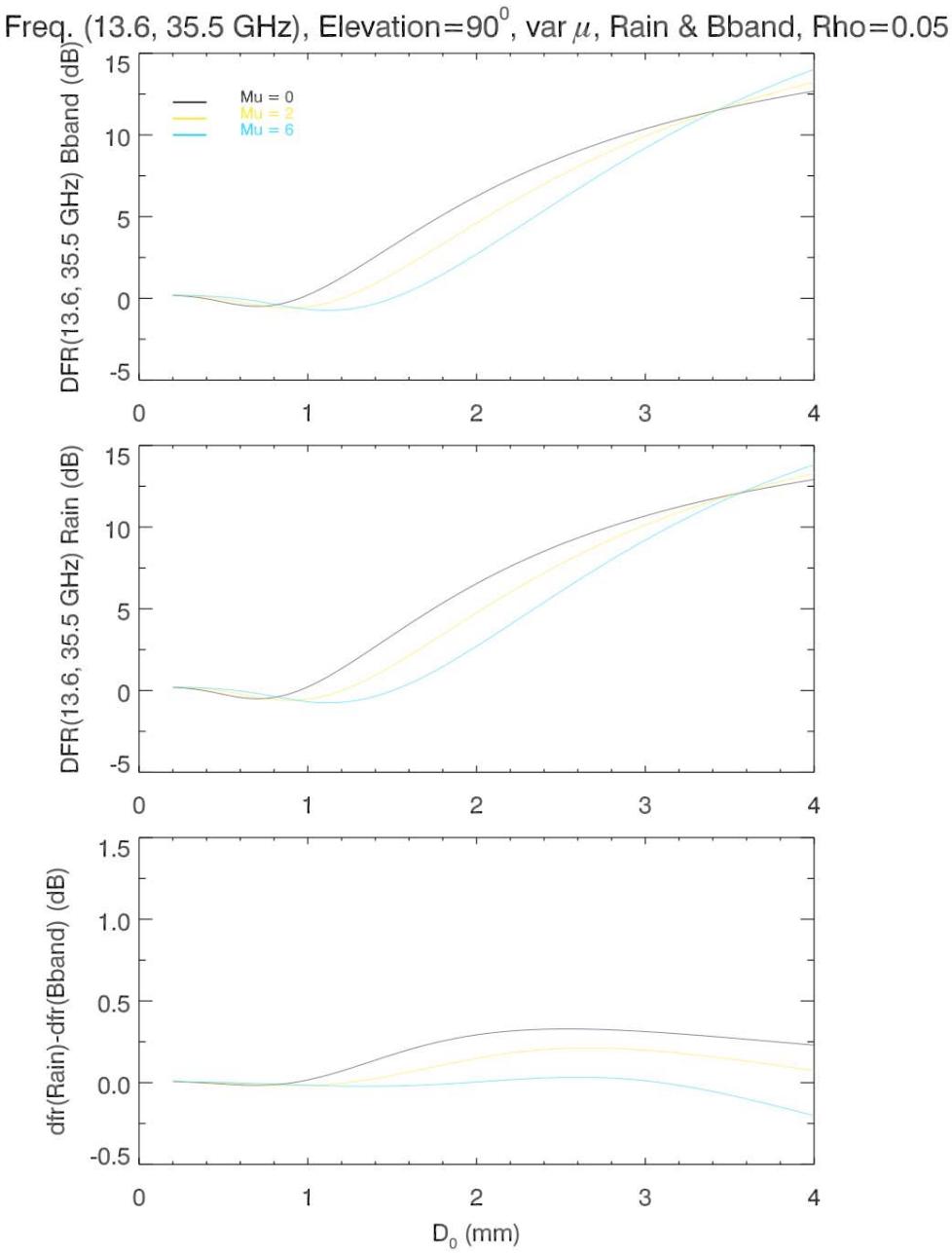
Freq. (13.6, 35.5 GHz), Elevation=90^0, var μ, Rain & Bband, Rho=0.05
Mu = 0
Mu = 2
Mu = 6
DFR(13.6, 35.5 GHz) Bband (dB)
DFR(13.6, 35.5 GHz) Rain (dB)
dfr(Rain)-dfr(Bband) (dB)
D_0 (mm)

Figure 11

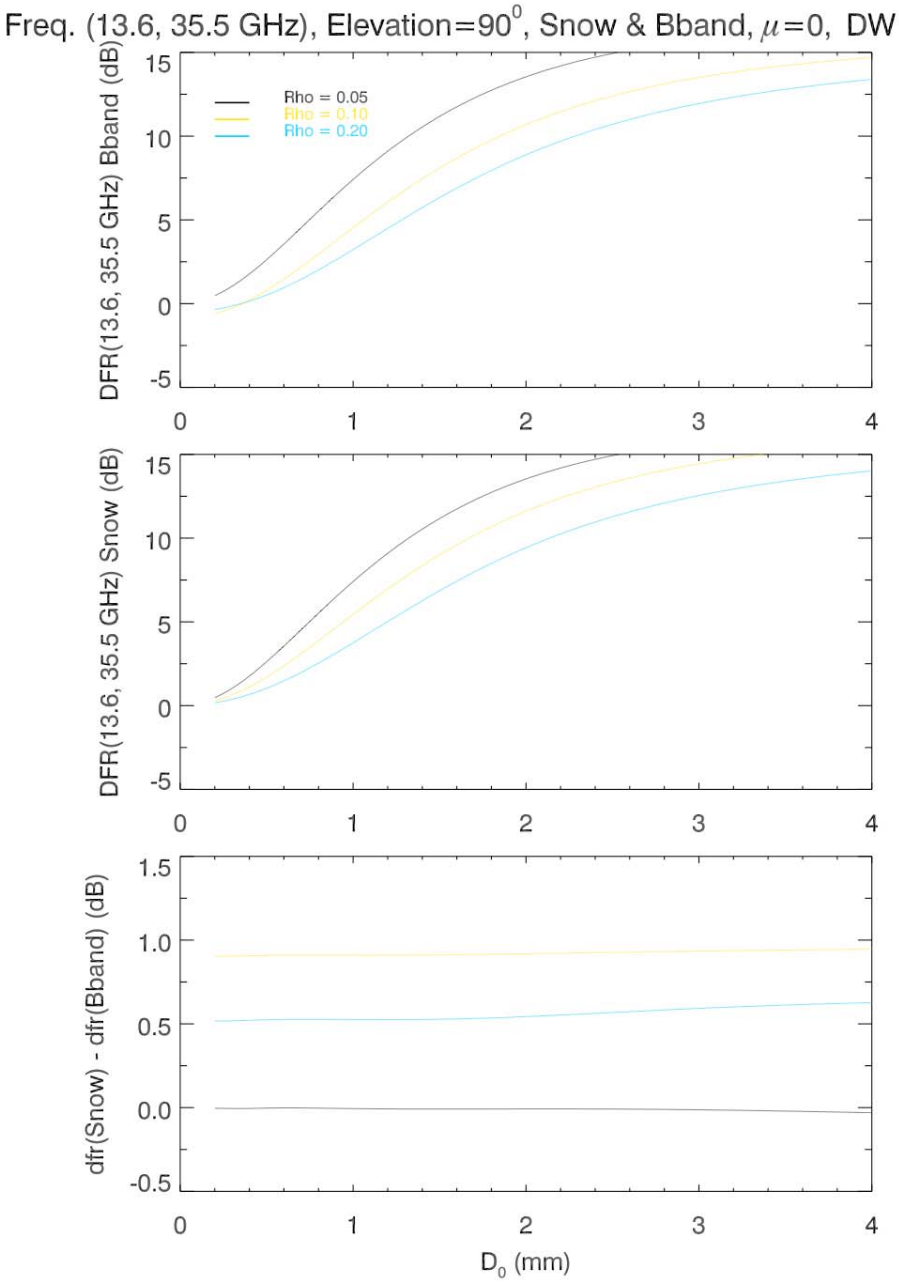
Freq. (13.6, 35.5 GHz), Elevation=90^0, Snow & Bband, μ=0, DW
Rho = 0.05
Rho = 0.10
Rho = 0.20
DFR(13.6, 35.5 GHz) Bband (dB)
DFR(13.6, 35.5 GHz) Snow (dB)
dfr(Snow) - dfr(Bband) (dB)
D_0 (mm)

7. Conclusion

The main goal of the backward recursion algorithm and data retrieval program is to take two equations and calculate two unknowns, D_0 and N_T. The program calculates these two particular DSD parameters because they have physical meaning. My focus was to explore different aspects of the program. First, I looked at how the retrieved parameters (D0, N_T, R) change as a function of variables such the shape factor, the dielectric constant, and the temperature. The changes in the DFR created by varying the dielectric constant and the temperature had almost no effect on the solutions produced by the retrieval program. The changes in the DFR created by varying μ had a significant effect on the solutions. The program overestimated or underestimated the D_0 and N_T values as μ varied. Second, I looked at areas where the model broke down. The one instance that I found where the model completely broke down is when N_T becomes very large. However, the N_T has to be unrealistically large for this to occur, and I could only produce the break down with simulated data. Lastly, I looked at expanding the retrieval program into other precipitation phases. I produced the look-up tables for the snow and the bright band at different density. Unfortunately, the look-up tables had some discrepancies between the rain, snow, and bright band; however, they did correspond well with each other for the most part. Overall, the backward recursion algorithm and data retrieval program look promising, but there are still some inaccuracies that need to be taken into account

In order to complete the data retrieval program, we need to accomplish several tasks. One task is that we need to determine which conventions are going to be used in the program. For example, should we use the variable or fixed dielectric constant? Should we define D_0 in terms of liquid water or in terms of snow? Should we just use D_m instead of D_0 because it is easier to calculate? Should we use a constant μ at every precipitation phase or should we vary the μ through the mixed phase? Another task is to determine where the mixed phase region begins and ends. Sometimes the bright band in the return power is clear and sometimes it can be very ambiguous. A third task is to establish how robust the data retrieval program will be. For example, should we include the rain look-up tables for the different temperature when it has such little effect on the solution? Should we include fail-safes for unlikely meteorological conditions? These are some of the tasks that must be completed before we implement the program, but, again, the backward recursion algorithm and data retrieval program look promising.

Work Cited

Battan, L. (1973). *Radar observation of the atmosphere.* Chicago: The University of Chicago Press.

Liao, L., & Meneghini, R. (2005, June). A study of air/space-borne dual-wavelength radar for estimation of rain profiles. *Advances in Atmospheric Sciences.*

Meneghini, R., Kozu, T., Kumagai, H., & Boncyk, W. (1992, August). Astudy of rain estimation methods from space using dual-wavelength radar measurement at near-nadir incidence over ocean. *Journal of Atmospheric and Oceanic Technology*.

Meneghini, R., Kumagai, H., Wang, J., Iguchi, T., & Kozu, T. (1997, May). Microphysical retrievals over stratiform rain using measurement from an airborne dual-wavelength radar-radiometer. *IEEE Transactions on Geoscience and Remote Sensing*.

Meneghini, R., & Liang Liao. (2006, August). On the equivalence of dual-wavelength and dual-polarization equations for estimation of the raindrop size distribution. *Journal of Atmospheric and Oceanic Technology*.

Rinehart, R. (2004). *Radar for meteorologists.* Fargo, ND: Knight Printing Company.

Testud, J. (Ed.). (2004). *Weather radar; Principles and advanced applications.* Germany: Springer.